Mycoscience VOL.65 (2024) 216–223

Mycoscience

An open access journal for general mycology

The Mycological Society of Japan

Full paper

Morphological responses of two *Aspergillus oryzae* strains to various metal ions at different concentrations

Liyun Liu[a], Kanae Sakai[a], Takumi Tanaka[a], and Ken-Ichi Kusumoto[a*]

[a] *Department of Biotechnology, Graduate School of Engineering, Osaka University, Yamada-oka 2-1, Suita, Osaka 565-0871, Japan*

ABSTRACT

Aspergillus species take up various metal ions from environment. The morphology of *Aspergillus oryzae* strains can vary under the influence of various metal ions. Here, the effects of Ti^{4+}, V^{3+}, Sr^{2+}, Ba^{2+}, Al^{3+}, Fe^{2+}, Zn^{2+}, Mn^{2+}, Ca^{2+}, and Cu^{2+} on morphological parameters of *A. oryzae* strains RIB40 and RIB143 were estimated. Colony diameter, conidiation, vesicle head size, and stipe width in both strains varied with concentration. Ti^{4+}, Sr^{2+}, Ba^{2+}, Al^{3+}, Fe^{2+}, and Ca^{2+} affected conidiation in similar tendency between two strains. The effects of Ti^{4+}, V^{3+}, Sr^{2+}, and Ba^{2+} on the morphology of *A. oryzae* are reported here for the first time. Induction of growth of both strains by 0.0001% Ti^{4+} may help the fermentation industry. Induction of conidiation in RIB40 by 0.001% Cu^{2+} confirmed previous results that low concentrations of Cu^{2+} promote the growth of *Aspergillus*. The most novel finding is that 0.001% Zn^{2+} increased the vesicle head size in RIB40; possible reasons are discussed.

Keywords: conidiation, metal ions, stipe width, vesicle head size

Article history: Received 26 February 2024, Revised 26 March 2024, Accepted 3 April 2024, Available online 23 August 2024.

1. Introduction

Minerals are released from rocks during soil formation via physical, chemical, and biological weathering processes (Hoffland et al., 2004; Kelly et al., 1998; Macheyeki et al., 2020). Physical weathering disintegrates the original primary minerals without changing their chemical composition, and chemical weathering converts them into secondary minerals (Macheyeki et al., 2020). Biological weathering dissolves minerals from rocks via acids secreted by organisms growing on the rocks (Hoffland et al., 2004; Kelly et al., 1998; Ribeiro et al., 2020). For instance, under favourable conditions, *Aspergillus niger* can secrete citric acid from its hyphal tips, to break down rock substrates (Hoffland et al., 2004), and thus constitutes an important component of the soil microbiota and ecosystems (Nayak et al., 2020).

Aspergillus species have high ability to take up various metal ions from the environment (Blatzer & Latgé, 2017; Ceci et al., 2012; Dusengemungu et al., 2020; Khani et al., 2012; Zhang et al., 2022). These metal ions play a significant role in the lives of filamentous fungi (Dusengemungu et al., 2020). For instance, Fe^{2+} takes part in vital biological mechanisms as a component of the electron transport chain, amino acid metabolism, and biosynthesis of DNA; Cu^{2+} and Zn^{2+} are incorporated into superoxide dismutase to protect against reactive oxygen species; Ca^{2+} belongs to cell wall functional groups; Mn^{2+} is essential for the growth of microorganisms (Bakti et al., 2018; Fejes et al., 2020; Haas, 2012; Latha et al., 2012). However, excessive Fe^{2+}, Cu^{2+}, Zn^{2+}, Ca^{2+}, or Mn^{2+} promote the formation of reactive oxygen species and damage cells (Haas, 2012; Krumova et al., 2016). Metal homeostasis in cells of *Aspergillus* is critical for its growth. The various environmental factors, including metal ions, may influence morphological forms in *Aspergillus* species.

Aspergillus oryzae can be isolated from plants, foods, and soils (El-Korany et al., 2020; Machida et al., 2008; Sahnoun et al., 2012). Various strains are widely used for production of fermented foods, enzymes, and secondary metabolites (Chang et al., 2014; Gomi, 2014; Nigam & Singh, 1999). *A. oryzae* can be classified into three groups (1–3) depending on the degree of deletion of aflatoxin biosynthesis genes (Kusumoto et al., 2000). Group 1 strains have few deletions while group 3 strains have deletion of the most of aflatoxin biosynthesis homologs (Kusumoto et al., 2000). It was supposed that group 1 strains are less domesticated than group 3 strains due to the less deletion degree of aflatoxin biosynthesis homologs (Kusumoto et al., 2000; Liu et al., 2023; Watarai et al., 2009). This different tendency of gene deletion between group 1 and group 3 strains may give different responses of two group strains to soil components (Liu et al., 2023).

We have found that one of soil components, humic acid stimulates or inhibits the growth of *A. oryzae* strains (Liu et al., 2023). Metal ions chelated by humic acid differentially affected giant colony diameter, stimulating it in strain RIB40 (Group 1) but not in strain RIB143 (Group 3), alone or mixed together (Liu et al., 2023). It was speculated that the chelated metal ions partly cause the dif-

* Corresponding author.
Ken-Ichi Kusumoto, Yamada-oka 2-1, Suita, Osaka 565-0871, Japan
E-mail address: kenichi_kusumoto@bio.eng.osaka-u.ac.jp

ferences in morphological response to humic acid in the strains. Al^{3+}, Ca^{2+}, Ti^{4+}, V^{3+}, Mn^{2+}, Fe^{2+}, Sr^{2+}, and Ba^{2+} are detected in commercial humic acid as chelated metal ions (Liu et al., 2023). Furthermore, it was accidently found that a low concentration of Cu^{2+} increased conidiation in RIB40 and deepened the conidial color in RIB143, and that Zn^{2+} extended the aerial hyphae in RIB40 (data not shown). These ten types of metal ions may affect morphological characters in *A. oryzae*. To evaluate the growth and morphological changes of *A. oryzae* in the presence of various metal ions, giant colony diameter, conidial number, vesical head size, and stipe width of RIB40 and RIB143 under different concentrations of Ti^{4+}, V^{3+}, Sr^{2+}, Ba^{2+}, Al^{3+}, Fe^{2+}, Zn^{2+}, Mn^{2+}, Ca^{2+}, and Cu^{2+} were determined.

2. Materials and Methods

2.1. Aspergillus oryzae strains and conidial collection

Strains RIB40 and RIB143 were obtained from the National Research Institute of Brewing, Higashi-Hiroshima, Japan. Both were grown in Czapek–Dox Agar (CDA) medium (Difco Laboratories Inc., Franklin Lakes, NJ, USA; 30 g/L sucrose, 3 g/L $NaNO_3$, 1 g/L K_2HPO_4, 0.5 g/L $MgSO_4$, 0.5 g/L KCl, 0.01 g/L $FeSO_4$) in 2% (w/v) agar. Water used for the media was pre-treated by reverse osmosis. After 13 d growth at 25 °C, conidia were collected by gently scraping the plate surface with a sterilized cell spreader in 0.8% (w/v) NaCl plus 0.1% (w/v) Tween 80. Following filtration at sterilized condition, the conidial suspension was washed with 0.1% (w/v) Tween 80 and stored in 25% (w/v) glycerol at −80 °C for later inoculation.

2.2. Addition of metal ions to growth medium

Ti^{4+}, V^{3+}, Sr^{2+}, Ba^{2+}, Al^{3+}, Fe^{2+}, Zn^{2+}, Mn^{2+}, Ca^{2+}, and Cu^{2+} were added individually to CDA medium at different concentrations (Table 1) before autoclaving. In the case of Fe^{2+}, the additional concentrations were separately indicated from original Fe^{2+} in CDA medium. The pH of the medium was adjusted to that of the control (CDA medium without the addition of metal ions) with 1 M KOH (Nacalai Tesque, Inc., Kyoto, Japan).

2.3. Determination of colony diameters and conidial numbers

Conidial stock solutions of RIB40 and RIB143 in glycerol were spread with a sterilized cotton swab on CDA medium and incubated at 30 °C for 14 d in the dark. Conidial suspensions were collected as in section 2.1., counted with a hemocytometer under a microscope (Optiphot-2, Nikon, Tokyo, Japan), and then diluted in sterilized Milli-Q water to 10^3 conidia/μL. 5 μL of suspension (containing 5×10^3 conidia) was spotted on the center of the plate and held the plate for 7 d at 30 °C. After incubation, the diameter of each giant colony was determined in four directions on day 7 and averaged. Conidia were collected as in section 2.1. and directly counted under a microscope (Optiphot-2) without filtration. Conidial density was calculated as conidial number per colony area = conidial number / π (average colony diameter / 2)^2 and presented as conidial number per mm^2; conidial number was presented as conidial number per plate.

2.4. Determination of vesical head size and stipe width

Vesicle head size and stipe width of aerial hyphae in slide cultures were determined. In brief, RIB40 and RIB143 were inoculated on the side of a square of CDA agar with or without metal ion supplementation (3 mm × 3 mm × 2 mm high) by a sterilized toothpick. The agar was set on a micro-slide glass (Matsunami Glass Ind., Ltd., Osaka, Japan) and covered with a micro-cover glass (Matsunami Glass) and held in a sterilized plate at 30 °C under 96%–99% relative humidity. The humidity was maintained by putting containers of water in the incubator, and measured by digital thermo-hygrometer (Waves Inc., Tokyo, Japan). After 3 d, a drop of lactophenol cotton blue stain (Muto Pure Chemical Co., Ltd., Tokyo, Japan) was placed on a clean micro-slide glass and carefully covered with the micro-cover glass removed from the agar. Slides were examined under a light microscope (Optiphot-2), and the vesicle head size and stipe width of the aerial hyphae (Supplemental Fig. S1) were determined with ToupView software (Hangzhou ToupTek Photonics, Zhejiang, China).

2.5. Statistical analysis

The results of 3 independent replicates for giant colony diameter, conidial density, and conidial number were analysed by two-tailed Student's *t*-test, and the relative values of three parameters were calculated as the ratio of treatment to control. The results of 10 records per slide for vesicle head size and stipe width were analysed by Tukey's test in an online box plot tool (BoxPlotR: http://shiny.chemgrid.org/boxplotr/). Significant differences were indicated as $^{*}P < 0.05$, $^{**}P < 0.01$, and $^{***}P < 0.001$. In bar graphs, values are presented as mean ± standard error (SE) of 3 replicates. In boxplot graphs, whiskers depict maximum and minimum without outliers, and the box depicts median, first, and third quartiles in 10 records of each slide. Dots are outliers.

3. Results and Discussion

The effects of 10 metal ions at two to four concentrations each on the vegetative growth, reproductive capacity, and morphological changes of *A. oryzae* strains RIB40 and RIB143 were tested. The vegetative growth capacity was assessed by giant colony diameter,

Table 1 Metal ion information for the current study.

Metal ion name	Symbol	Added chemical	Company information of chemical	Concentration (w/v)				
Titanium	Ti^{4+}	$Ti(SO_4)_2$	Kanto Chemical Co., Inc., Tokyo, Japan	0%,	0.0001%,	0.001%		
Vanadium	V^{3+}	$V(NO_3)_3$	Kanto Chemical Co., Inc., Tokyo, Japan	0%,	0.001%,	0.01%,		
Strontium	Sr^{2+}	$Sr(NO_3)_2$	Nacalai Tesque, Inc., Kyoto, Japan	0%,	0.001%,	0.01%,	0.1%	
Barium	Ba^{2+}	$Ba(NO_3)_2$	Nacalai Tesque, Inc., Kyoto, Japan	0%,	0.0001%,	0.001%,	0.01%	
Aluminum	Al^{3+}	$Al(NO_3)_3$	Kanto Chemical Co., Inc., Tokyo, Japan	0%,	0.001%,	0.01%,		
Iron	Fe^{2+}	$FeSO_4$	Nacalai Tesque, Inc., Kyoto, Japan	0%,	0.001%,	0.01%,	0.1%	
Zinc	Zn^{2+}	$ZnSO_4$	Nacalai Tesque, Inc., Kyoto, Japan	0%,	0.00001%,	0.0001%,	0.001%,	0.01%
Manganese	Mn^{2+}	$Mn(NO_3)_2$	Wako Pure Chemical Industries, Ltd., Osaka, Japan	0%,	0.001%,	0.01%,	0.1%	
Calcium	Ca^{2+}	$CaCl_2$	Wako Pure Chemical Industries, Ltd., Osaka, Japan	0%,	0.001%,	0.01%,	0.1%	
Copper	Cu^{2+}	$CuSO_4$	Wako Pure Chemical Industries, Ltd., Osaka, Japan	0%,	0.001%,	0.01%,	0.1%	

reproductive capacity was assessed by conidiation (conidial number), and morphological change was assessed by vesicle head size and stipe width of conidiophores responding to metal ions. Low to moderate concentrations of individual metal ions brought different effects on giant colony diameter (Fig. 1; Supplemental Figs. S2, S3), conidiation (as conidial number; Fig. 2), vesicle head size (Fig. 3), and stipe width of aerial hyphae (Fig. 4).

3.1. Effects of metal ions on giant colony diameter and conidiation

Studies involved in Ti^{4+} and *Aspergillus* species mostly focused on the photocatalytic activity of TiO_2 (nanoparticle) (Babaei et al., 2016; Yang et al., 2023), and TiO_2 inhibited the growth of *Aspergillus flavus* (closely related species of *A. oryzae*) at 0.1% with UV irradiation (Babaei et al., 2016). However, direct effect of Ti^{4+} on the growth of *A. oryzae* is not known. The stimulative effect of 0.0001% Ti^{4+} on the vegetative growth and conidial number (Figs. 1, 2) of *A. oryzae* (RIB40 and RIB143) here is the first finding.

The removal of V^{3+} and Sr^{2+} from the environment by *Aspergillus* species is a common focus in studies (Pan et al., 2009; Mirazimi et al., 2015; Rasoulnia & Mousavi, 2016), and no information about related studies between *Aspergillus* species and Ba^{2+}, even this metal is the 14th most abundant element in Earth's crust (Cappuyns, 2018). The effect of V^{3+}, Sr^{2+} and Ba^{2+} on the morphological characteristics of *A. oryzae* is not known. The stimulative effects of 0.01% V^{3+} and 0.01% Sr^{2+} on the vegetative growth capacity of RIB40 (Fig. 1A), 0.1% Sr^{2+} on the vegetative growth capacity of RIB143, and stimulative effects of 0.001% V^{3+} on the reproductive capacity in RIB40 (Fig. 2B) were the first findings. Other concentrations of V^{3+} and Sr^{2+} inhibited or unaltered on the vegetative and reproductive capacities in RIB40 or RIB143 (Figs. 1, 2). All tested concentrations of Ba^{2+} stimulated the vegetative growth capacity in RIB40, whereas 0.01% Ba^{2+} inhibited it in RIB143 (Fig. 1). Additionally, 0.001 % and 0.01 % Ba^{2+} inhibited the reproductive capacity in both strains (Fig. 2).

Al^{3+} occurs commonly in acidic soils (He et al., 2019). It was reported that *A. oryzae* (isolated from the River Nile, Luxor, Egypt) showed tolerance against 0.0001% to 0.1% of Al^{3+} (Mahmoud et al., 2017). In this study, 0.001% Al^{3+} stimulated the vegetative growth of RIB40 (Fig. 1A), and instead, 0.01% Al^{3+} decreased the vegetative growth capacity and reproductive capacity in RIB40 and RIB143 (Figs. 1, 2). Here is the first to report about reproductive capacities of *Aspergillus* species at different concentrations of Al^{3+}. Our results of the vegetative growth and conidiation capacities of both strains under different concentrations of Ti^{4+}, V^{3+}, Sr^{2+}, Ba^{2+}, and Al^{3+} may provide useful information for further study of the effects of these metal ions in *Aspergillus* species.

Fe^{2+} is a critical micronutrient for the growth and survival of most microorganism (Frawley & Fang, 2014; Haas, 2012). The tolerance of the *A. oryzae* strain to the concentrations of Fe^{2+} from 0.0001% to 0.01% was reported (Mahmoud et al., 2017). In the present result, the additional 0.001% Fe^{2+} stimulated the vegetative growth capacity of RIB40 and RIB143, but the additional 0.1% reduced it (Fig. 1). The reason of the stimulative effect of 0.001% Fe^{2+} on the growth of RIB40 and RIB143 should be further analysed.

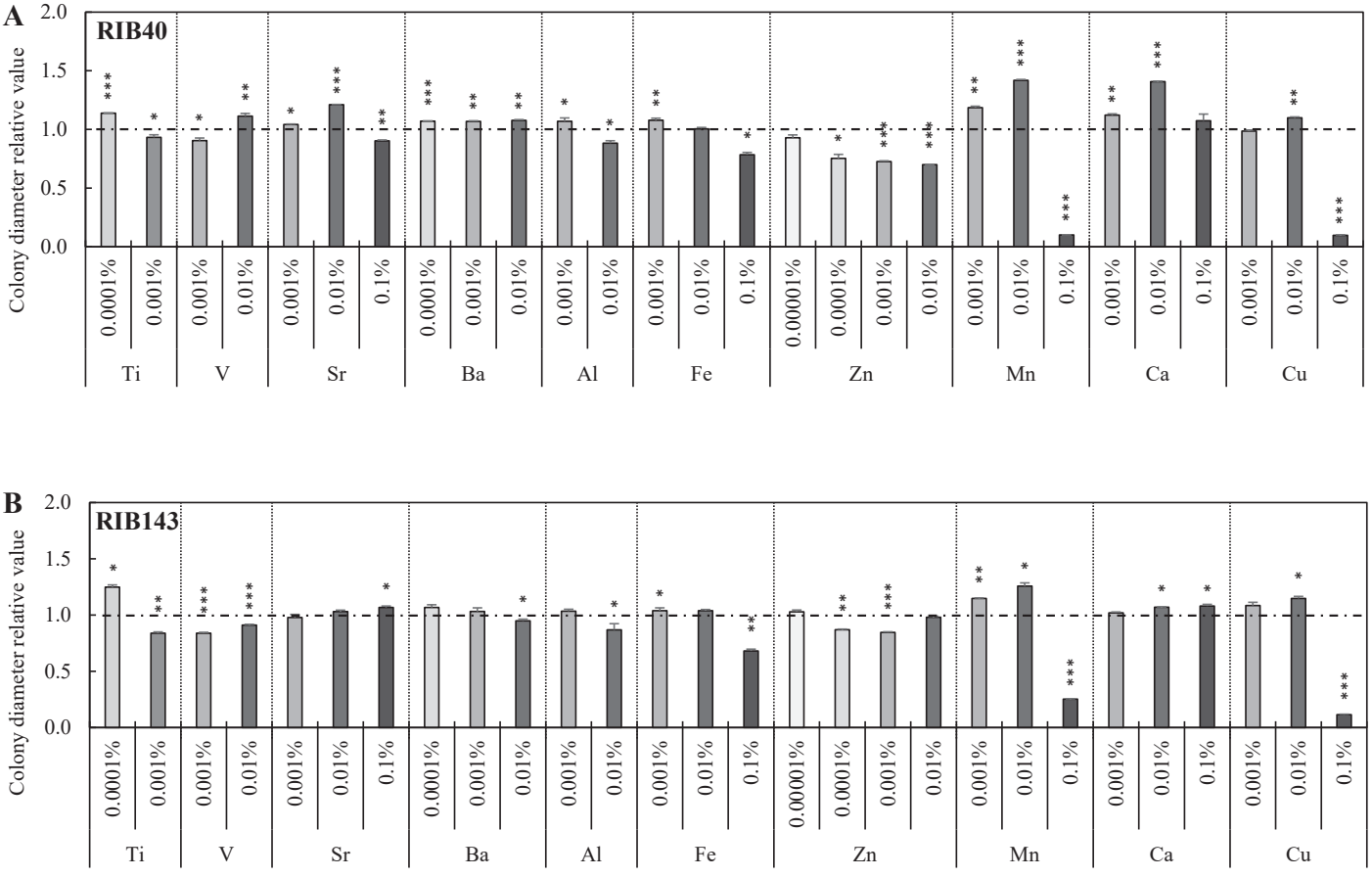

Fig. 1 – Giant colony diameter relative values of *Aspergillus oryzae* RIB40 and RIB143 treated with different concentrations of metal ions, including Ti^{4+}, V^{3+}, Sr^{2+}, Ba^{2+}, Al^{3+}, Fe^{2+}, Zn^{2+}, Mn^{2+}, Ca^{2+}, and Cu^{2+}. Control was set as 1. The relative value was calculated as the follow: relative value = colony diameter of treatment/colony diameter of control. Diameters were measured after 7 d growth at 30 °C. Results are means ± standard error (SE) ($n = 3$). Asterisks indicate significant differences ($^{*}P < 0.05$, $^{**}P < 0.01$, $^{***}P < 0.001$).

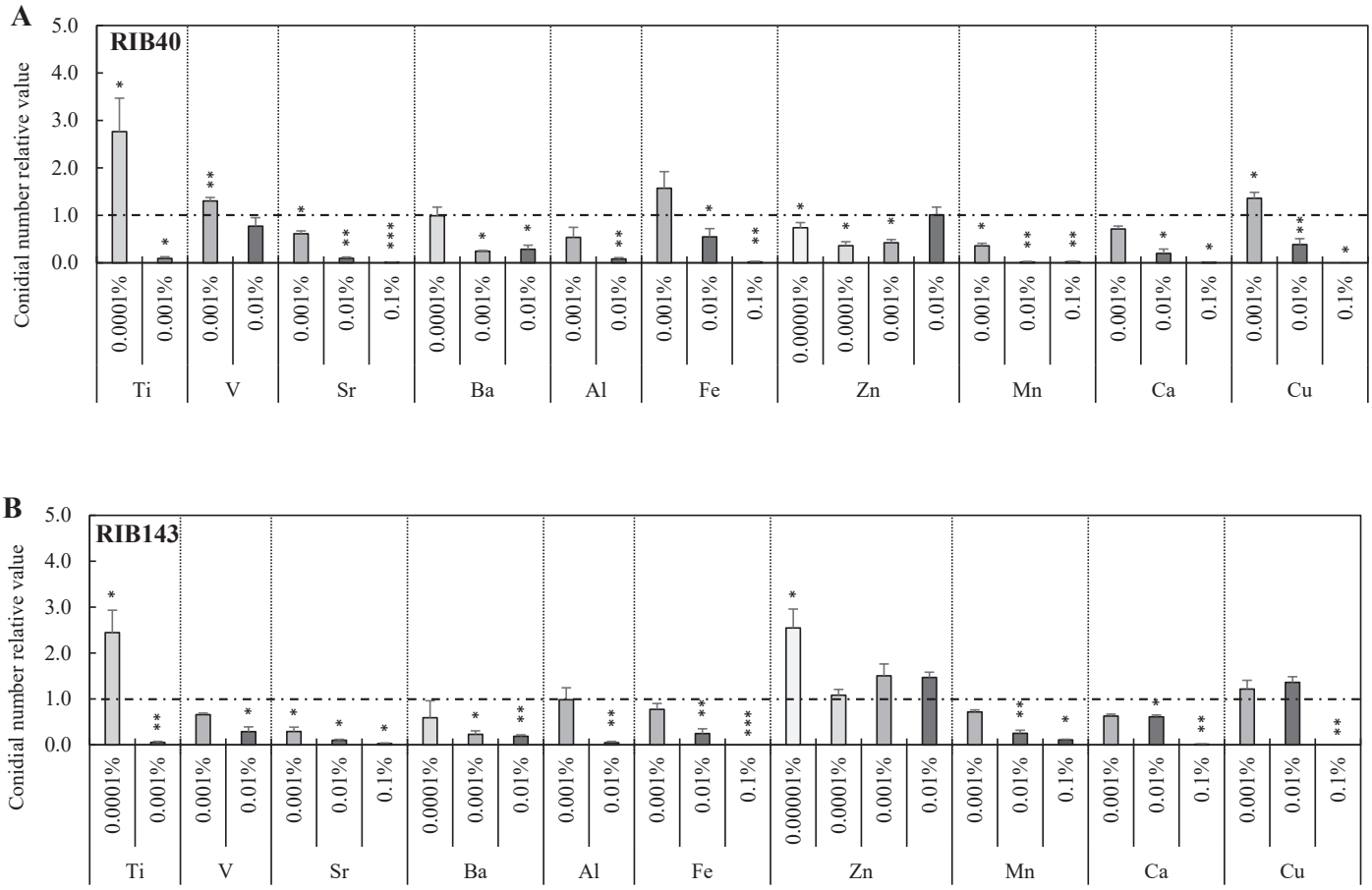

Fig. 2 – Conidial number relative values of *Aspergillus oryzae* RIB40 and RIB143 per plate treated with different concentrations of metal ions, including Ti^{4+}, V^{3+}, Sr^{2+}, Ba^{2+}, Al^{3+}, Fe^{2+}, Zn^{2+}, Mn^{2+}, Ca^{2+}, and Cu^{2+}. Control was set as 1. The relative value was calculated as the follow: relative value = conidial number of treatment/ conidial number of control. Conidia were counted after 7 d growth at 30 °C. Results are means ± standard error (SE) ($n = 3$). Asterisks indicate significant differences ($^{*}P < 0.05$, $^{**}P < 0.01$, $^{***}P < 0.001$).

Excessive Fe^{2+} has potential to promote the formation of reactive oxygen species and damage cells (Haas, 2012). The reason of the inhibitive effect of 0.1% Fe^{2+} on the growth of two strains may be the over-production of relative oxygen species in the cells. The yellow color of CDA medium containing 0.1% Fe^{2+} is the original color of the medium before inoculating the strains and may be the one of ferric oxide.

Zn^{2+} is the second most abundant transition micronutrient required by microorganisms and is essential for biochemical processes, cellular growth, and development (Amich & Calera, 2014). Hartikainen et al. (2012) reported that Zn^{2+} at 100, 200 and 400 mg/kg (0.01 – 0.04%) (contained on malt extract agar plate) decreased the most growth of some saprotrophic fungi (Basidiomycete, Ascomycete and Zygomycete) (Hartikainen et al. 2012). The only exception within ascomycete and zygomycete was the increased growth of *Coniothyrium* sp. with the same concentration of Zn^{2+} (Hartikainen et al. 2012). They also described that several Basidiomycete fungi increased their growth with the same concentration of Zn^{2+}. In this study, most concentrations of Zn^{2+} inhibited the vegetative capacity in RIB40 and RIB143, and it showed a concentration-independent tendency (Fig. 1). In addition, Lanfranco et al. (2002) reported that Zn^{2+} affected the growth and morphology of the ericoid symbiotic fungus, led to apical swellings, and increased branching in the sub-apical parts. The length of aerial hyphae of RIB40 increased by Zn^{2+}, and the colony of RIB40 was dense and fluffy along with increasing Zn^{2+} concentration (Supplemental Fig. S2). The mycelial dense within the colony of RIB143 was observed as well, but fluffy was not observed in RIB143 responding to Zn^{2+}. RIB40 may change its hyphal fluffiness responding to Zn^{2+}, besides RIB143 may not, probably due to the difference of the gene set.

Mn^{2+} are essential for the growth of microorganisms (Fejes et al., 2020). Mn^{2+} from 0.0001% to 0.1% unaltered the growth of *A. oryzae* strain (Mahmoud et al., 2017). However, in this study, Mn^{2+} gradually stimulated the vegetative growth capacity from 0.001% to 0.01%, and sharply inhibited it at 0.1% in two strains (Fig. 1). In addition, Mn^{2+} (0.001%, 0.01%, and 0.1%) decreased conidial number, however, 0.1% Mn^{2+} recovered conidial density because of the serious reduction of giant colony diameter in RIB40 (Figs. 1A, 2A; Supplementary Fig. S4).

Binding of Ca^{2+} to cell wall functional groups as a macronutrient supports the growth of microorganisms (Latha et al., 2012). For instance, Ca^{2+} affects growth, hyphal morphology, and citric acid production in *A. niger* (Pera & Callieri, 1997). Here, Ca^{2+} stimulated colony growth at 0.001% and significantly at 0.01% in RIB40, and at 0.01% and 0.1% in RIB143 (Fig. 1; Supplemental Figs. S2, S3). However, significantly inhibited reproductive capacity (Fig. 2; Supplemental Fig. S4) at 0.01% and 0.1%. Therefore, Ca^{2+} stimulated hyphal growth but inhibited reproductive capacity. The reason of stimulative effects of Ca^{2+} on hyphal growth was not clear. The inhibitive effects of Ca^{2+} on reproductive capacity might be due to reduced expression of some Ca^{2+} transporters which involved in asexual conidiation (Wang et al., 2021).

Cu^{2+} is a cofactor of antioxidant enzymes such as laccase and superoxide dismutase (Raffa et al., 2019). Hartikainen et al. (2012)

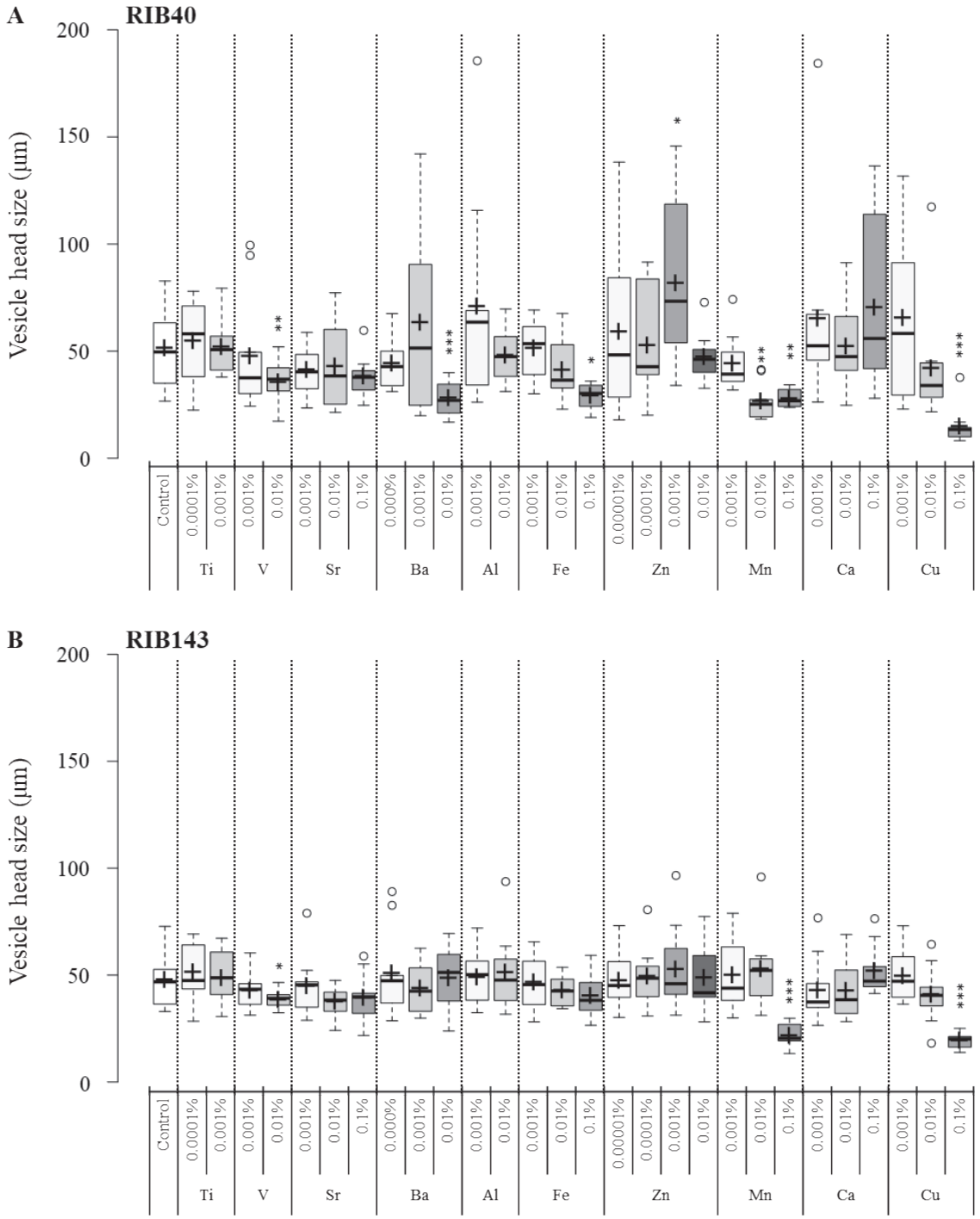

Fig. 3 – Box plots of vesicle head sizes of *Aspergillus oryzae* RIB40 and RIB143 after 3 d growth at 30 °C with different concentrations of metal ions. Whiskers depict maximum and minimum without outliers, and the box depicts median and first and third quartiles. Dots are outliers. Asterisks indicate significant differences between control and treatment ($^{*}P < 0.05$, $^{**}P < 0.01$, $^{***}P < 0.001$, $n = 10$).

reported that most of the 18 strains of fungi decreased their growth with 100–400 mg/kg (0.01–0.04%) of Cu^{2+}, with the exception of one Basidiomycete. In *A. oryzae*, Cu^{2+} regulates conidiation via Cu^{2+}-dependent superoxide dismutase and induces conidiation (Katayama & Maruyama, 2023). Therefore, incorporation of Cu^{2+} into superoxide dismutase to act against reactive oxygen species may explain the induction of conidiation in RIB40 by 0.001% Cu^{2+}. Excessive Cu^{2+} (0.1%) may have caused intercellular toxicity and the inhibition of growth and conidiation in RIB40 and RIB143 (Figs. 1, 2). This toxic effect of 0.1% Cu^{2+} on growth of filamentous fungi is also observed in *A. fumigatus* (Krumova et al., 2016).

3.2. Effects of metal ions on vesical head size and stipe width

High concentrations of V^{3+} (0.01%), Mn^{2+} (0.1%), and Cu^{2+} (0.1%) decreased vesical head size in RIB40 and RIB143 (Fig. 3). High concentration of Ba^{2+} (0.01%), Fe^{2+} (0.1%), and moderate concentration of Mn^{2+} (0.01%) only decreased vesical head size in RIB40 (Fig. 3A). High concentrations of Sr^{2+} (0.1%), Mn^{2+} (0.1%), and Cu^{2+} (0.1%) decreased stipe width in RIB40 and RIB143 (Fig.

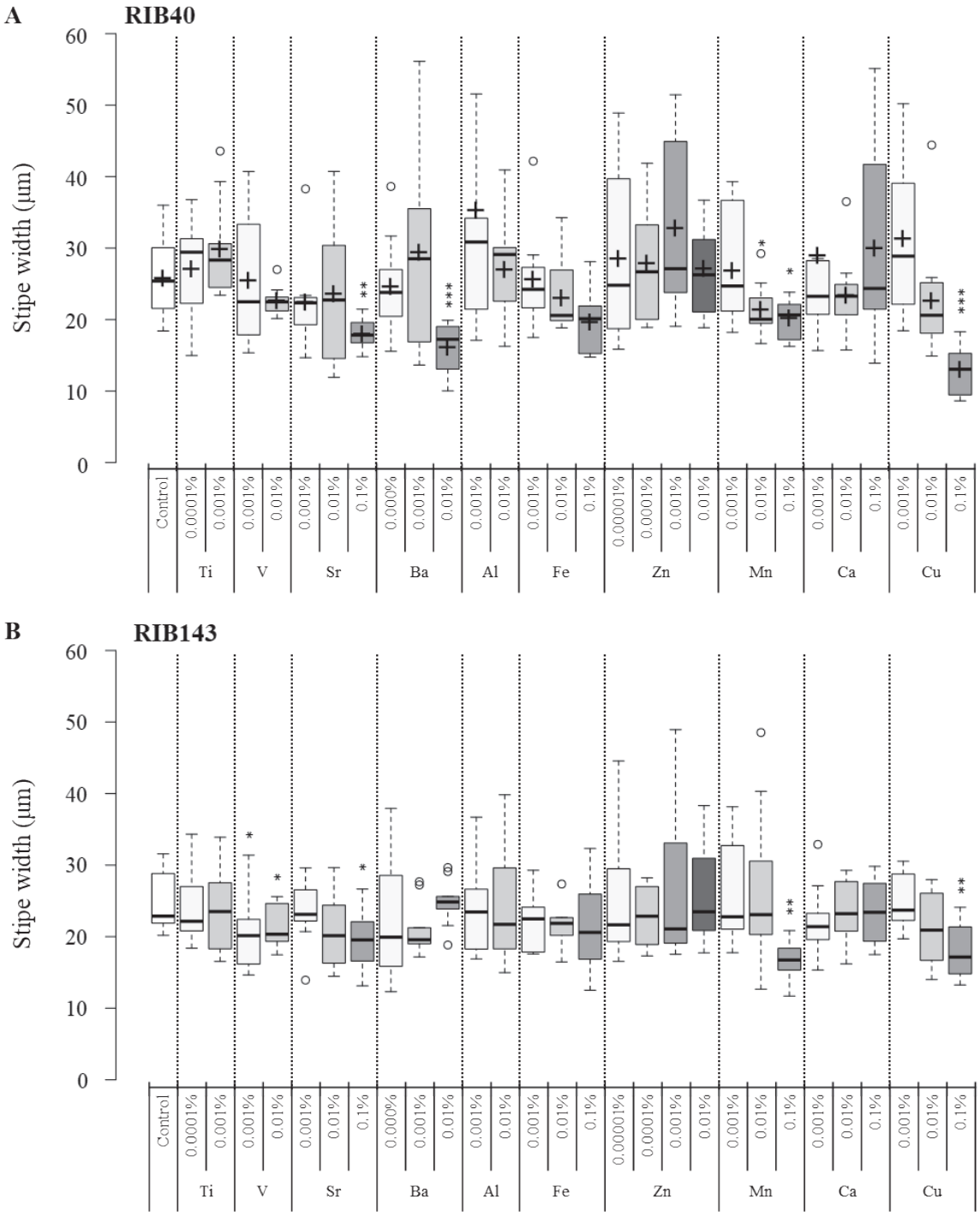

Fig. 4 – Box plots of widths of stipes directly connected with vesicles of *Aspergillus oryzae* RIB40 and RIB143 after 3 d growth at 30 °C with different concentrations of metal ions. Whiskers depict maximum and minimum without outliers, and the box depicts median and first and third quartiles. Dots are outliers. Asterisks indicate significant differences between control and treatment ($^{*}P < 0.05$, $^{**}P < 0.01$, $^{***}P < 0.001$, $n = 10$).

4). High concentration of Ba^{2+} (0.01%) and moderate concentration of Mn^{2+} (0.01%) only decreased stipe width in RIB40 (Fig. 4A). High concentrations of V^{3+} (0.001%, 0.01%) only decreased stipe width in RIB143 (Fig. 4B). Other metal ions did not affect vesical head size and stipe width in RIB40 or RIB143 at any concentrations (Figs. 3, 4).

Specially, 0.001% Zn^{2+} stimulated vesicle head size in RIB40 (Fig. 3A; Supplemental Fig. S5). The BrlA transcription factor is known to control the initiation of aerial hyphal development, including development of vesicles, metuale, phialides, and conidia (Yu, 2010). Zn^{2+} is important for forming a C_2H_2 zinc finger DNA-binding domain in BrlA (Wu et al., 2018). It is bold to suppose that the addition of 0.001% Zn^{2+} to growth medium disturbed the regulation network of *brlA* and further affected vesicle head size in RIB40. One explanation for the stimulation of vesicle head size by 0.001% Zn^{2+} is that some enzymes or signalling proteins involved in the development of the vesicle head may interact with zinc, i.e., having a zinc binding protein in the case of RIB40 but not in RIB143. Clarifying the genetic differences between RIB40 and RIB143 may identify genes related to vesicle head development in

A. oryzae. Our findings may contribute new tools with which to clarify the mechanism of conidial head development in fungi.

Overall, the addition of metal ions to CDA medium was separated to six sets (Ti^{4+} and Ba^{2+}, V^{3+} and Sr^{2+}, Al^{3+} and Fe^{2+}, Ca^{2+} and Cu^{2+}, Zn^{2+}, Mn^{2+}), due to the limitation of the incubation space. The relative value of each parameter in Fig 1 and Fig. 2 was calculated as the ratio of treatment to control. Therefore, the results of relative value were not affected by the true values of each parameter in Fig. 1 and Fig. 2. Ti^{4+}, Fe^{2+}, Mn^{2+}, and Cu^{2+} affected the relative value of colony diameter (Fig. 1); Ti^{4+}, Sr^{2+}, Ba^{2+}, Al^{3+}, Fe^{2+}, and Ca^{2+} affected the relative value of conidial number (Fig. 2); V^{3+} and Cu^{2+} affected vesicle head size (Fig. 3); and Sr^{2+} and Cu^{2+} affected stipe width (Fig. 4) in similar tendency between two strains. However, V^{3+}, Sr^{2+}, Ba^{2+}, Al^{3+}, Mn^{2+}, Ca^{2+}, and Cu^{2+} affected morphology more in RIB40 than in RIB143. Domestication modifies morphological, physiological, and genetic characteristics (Steensels et al., 2019). According to the degree of aflatoxin biosynthesis homologs gene deletion, RIB143 is thought to be more domesticated strain than RIB40 (Kusumoto et al., 2000), and thus the mutation of genes in RIB143 during its domestication may explain the difference in morphology between RIB143 and RIB40 in response to these metal ions. It was supposed that the gene functions sensing or responding to metal ions in the environment may have more disappeared or weakened in RIB143 during the domestication from environmental strain. It should be interesting to identify and investigate some genes or signal pathways causing the different response to *A. oryzae* strains to these metal ions.

4. Conclusion

This study was conducted to estimate the influence of varied metal ions on the morphology of two *A. oryzae* strains, RIB40 and RIB143. This study firstly reported the morphology of RIB40 and RIB143 responding to Ti^{4+}, V^{3+}, Sr^{2+}, Ba^{2+}, and Zn^{2+}. Increased growth of two strains by 0.0001% Ti^{4+} is a novel point, while increased vesicle head size in RIB40 by 001% Zn^{2+} provided the most novel finding in this study.

Disclosure

All authors declare no conflicts of interest.

Acknowledgements

This study was supported by the Institute for Fermentation, Osaka, Japan, under grant number K-2021-008.

References

Amich, J., & Calera, J.A. (2014). Zinc acquisition: a key aspect in *Aspergillus fumigatus* virulence. *Mycopathologia, 178*, 379–385. https://doi.org/10.1007/s11046-014-9764-2

Babaei, E., Dehnad, A., Hajizadeh, N., Valizadeh, H., & Reihani, S.F.S. (2016). A study on inhibitory effects of titanium dioxide nanoparticles and its photocatalytic type on *Staphylococcus aureus*, *Escherichia coli* and *Aspergillus flavus*. *Applied Food Biotechnology 3*, 115–123. https://doi.org/10.22037/afb.v3i2.10571

Bakti, F., Sasse, C., Heinekamp, T., Pócsi, I., & Braus, G.H. (2018). Heavy metal-induced expression of PcaA provides cadmium tolerance to *Aspergillus fumigatus* and supports its virulence in the *Galleria mellonella* model. *Frontiers in Microbiology 9*, 744. https://doi.org/10.3389/fmicb.2018.00744

Blatzer, M., & Latgé, J.P. (2017). Metal-homeostasis in the pathobiology of the opportunistic human fungal pathogen *Aspergillus fumigatus*. *Current Opinion in Microbiology 40*, 152–159. https://doi.org/10.1016/j.mib.2017.11.015

Cappuyns, V. (2018). Barium (Ba) leaching from soils and certified reference materials. *Applied Geochemistry 88*, 68–84. https://doi.org/10.1016/j.apgeochem.2017.05.002

Ceci, A., Maggi, O., Pinzari, F., & Persiani, A.M. (2012). Growth responses to and accumulation of vanadium in agricultural soil fungi. *Applied Soil Ecology 58*, 1–11. https://doi.org/10.1016/j.apsoil.2012.02.022

Chang, P.K., Horn, B.W., Abe, K., & Gomi, K. (2014). *Aspergillus*/Introduction. In: C.A.Batt, M.L. Tortorello (Eds.), *Encyclopedia of Food Microbiology* (pp.77–82). https://doi.org/10.1016/B978-0-12-384730-0.00010-0

Dusengemungu, L., Kasali, G., Gwanama, C., & Ouma, K.O. (2020). Recent advances in biosorption of copper and cobalt by filamentous fungi. *Frontiers in Microbiology 11*, 582016. https://doi.org/10.3389/fmicb.2020.582016

El-Korany, S.M., Helmy, O.M., El-Halawany, A.M., Ragab, Y.E.M., & Zedan, H.H. (2020). Kojic acid repurposing as a pancreatic lipase inhibitor and the optimization of its production from a local *Aspergillus oryzae* soil isolate. *BMC Biotechnology 20*, 52. https://doi.org/10.1186/s12896-020-00644-9

Fejes, B., Ouedraogo, J.P., Fekete, E., Sándor, E., Flipphi, M., Soós, Á., Molnár, Á.P., Kovács, B., Kubicek, C.P., Tsang, A., & Karaffa, L. (2020). The effects of external Mn^{2+} concentration on hyphal morphology and citric acid production are mediated primarily by the NRAMP-family transporter DmtA in *Aspergillus niger*. *Microbial cell factories 19*, 17. https://doi.org/10.1186/s12934-020-1286-7.

Frawley, E.R., & Fang, F.C. (2014) The ins and outs of bacterial iron metabolism. *Mol. Microbiol.* 93, 609–616.

Gomi, K. (2014). *Aspergillus/ Aspergillus oryzae*. In: C.A.Batt, M.L. Tortorello (Eds.), *Encyclopedia of Food Microbiology* (pp. 92–96). https://doi.org/10.1016/B978-0-12-384730-0.00011-2

Hartikainen, E.S., Lankinen, P., Rajasärkkä, J., Koponen, H., Virta, M., Hatakka, A., & Kähkönen, M.A. (2012). Impact of copper and zinc on the growth of saprotrophic fungi and the production of extracellular enzymes. *Boreal Environment Research* 17, 210–218.

Haas, H. (2012). Iron – a key nexus in the virulence of *Aspergillus fumigatus*. *Frontiers in Microbiology 3*, 28. https://doi.org/10.3389/fmicb.2012.00028

He, H., Li, Y., & He, L.F. (2019). Aluminum toxicity and tolerance in Solanaceae plants. *South African Journal of Botany 123*, 23–29. https://doi.org/10.1016/j.sajb.2019.02.008

Hoffland, E., Kuyper, T.W., Wallander, H., Plassard, C., Gorbushina, A.A., Haselwandter, K., Holmström, S., Landeweert, R., & Landeweert, R. (2004). The role of fungi in weathering. *Frontiers in Ecology and the Environment 2*, 258–264. https://doi.org/10.1890/1540-9295(2004)002[0258:TROFIW]2.0.CO;2

Katayama, T., & Maruyama, J. (2023). Trace copper-mediated asexual development via a superoxide dismutase and induction of *AobrlA* in *Aspergillus oryzae*. *Frontiers in Microbiology 14*, 1135012. https://doi.org/10.3389/fmicb.2023.1135012

Kelly, E., Chadwick, O.A., & Hilinski, T.E. (1998). The effect of plants on mineral weathering.*Biogeochemistry42*,21–53.https://doi.org/10.1023/A:1005919306687

Khani, M.H., Pahlavanzadeh, H., & Alizadeh, K. (2012). Biosorption of strontium from aqueous solution by fungus *Aspergillus terreus*. *Environmental Science and Pollution Research 19*, 2408–2418. https://doi.org/10.1007/s11356-012-0753-z

Krumova, E., Kostadinova, N., Miteva-Staleva, J., Gryshko, V., & Angelova, M. (2016). Cellular response to Cu- and Zn-induced oxidative stress in *Aspergillus fumigatus* isolated from polluted soils in Bulgaria. *Clean–Soil, Air, Water 44*, 657–666. https://doi.org/10.1002/clen.201500139

Kusumoto, K.I., Nogata, Y., & Ohta, H. (2000). Directed deletions in the aflatoxin biosynthesis gene homolog cluster of *Aspergillus oryzae*. *Current Genetics 37*, 104–111. https://doi.org/10.1007/s002940050016

Lanfranco, L., Balsamo, R., Martino, E., Perotto, S., & Bonfante, P. (2002). Zinc ions alter morphology and chitin deposition in an ericoid fungus. *Eur. J. Histochem. 46*, 341–350. https://doi.org/10.4081/1746

Latha, J. N. L., Babu, P. N., Rakesh, P., Kumar, K. A., Anupama, M., & Susheela L. (2012). Fungal cell walls as protective barriers for toxic metals. *Advances in Medicine and Biology 53*, 181–198.

Liu, L., Sakai, K., Tanaka, T., & Kusumoto, K. (2023). Subcomponents in humic acid structure contribute to the differential responses of *Aspergillus oryzae* strains to humic acid. https://doi.org/10.2323/jgam.2023.07.003

Macheyeki, A.S., Li, X., Kafumu, D.P., & Yuan, F. (2020). Elements of exploration geochemistry. In: A. S. Macheyeki, X. Li, D. P. Kafumu, F. Yuan (Eds.), *Applied Geochemistry: Advances in Mineral Exploration Techniques* (pp. 1–43). https://doi.org/10.1016/B978-0-12-819495-9.00001-3

Machida, M., Yamada, O., & Gomi, K. (2008). Genomics of *Aspergillus oryzae*: learning from the history of koji mold and exploration of its future. *DNA Research 15*, 173–183. https://doi.org/10.1093/dnares/dsn020

Mahmoud, A.H., Massoud, M.S., Abdel-Motaal, F.F., & El-Zayat, S.A. (2017). Tolerance and biosorption of manganese, iron and aluminum by five *Aspergillus* species isolated from freshwater. *Catrina 16*, 61–69

Mirazimi, S.M.J., Abbasalipour, Z., & Rashchi, F. (2015). Vanadium removal from LD converter slag using bacteria and fungi. *Journal of Environmental Management 153*, 144–151. https://doi.org/10.1016/j.jenvman.2015.02.008

Nayak, S., Samanta, S., & Mukherjee, A.K. (2020). Beneficial role of *Aspergillus sp.*

in agricultural soil and environment. In: S. Nayak, S. Samanta, A. K. Mukherjee (Eds.) *Frontiers in Soil and Environmental Microbiology* (pp. 17–36).

Nigam, P., & Singh, D. (1999). Metabolic pathways/ Production of secondary metabolites-Fungi. In: R. K. Robinson (Eds.), *Encyclopedia of Food Microbiology* (pp. 1319–1328). https://doi.org/10.1006/rwfm.1999.1012

Pan, X., Meng, X., Zhang, D., & Wang. J. (2009). Biosorption of strontium ion by immobilized *Aspergillus niger*. *International Journal of Environment and Pollution 37*, 276–288. https://doi.org/10.1504/IJEP.2009.025131

Pera, L.M., & Callieri, D.A. (1997). Influence of calcium on fungal growth, hyphal morphology and citric acid production in *Aspergillus niger*. *Folia Microbiol. 42*, 551–556. https://doi.org/10.1007/BF02815463

Raffa, N., Osherow, N., & Keller, N.P. (2019). Copper utilization, regulation, and acquisition by *Aspergillus fumigatus*. *International Journal of Molecular Sciences 20*, 1980. https://doi.org/10.3390/ijms20081980

Rasoulnia, P., & Mousavi, S.M. (2016). V and Ni recovery from a vanadium-rich power plant residual ash using acid producing fungi: *Aspergillus niger* and *Penicillium simplicissimum*. *RSC Advances 6*, 9139. https://doi.org/10.1039/C5RA24870A

Ribeiro, I.D.A., Volpiano, C.G., Vargas, L.K., Granada, C.E., Lisboa, B.B., & Passaglia, L.M.P. (2020). Use of mineral weathering bacteria to enhance nutrient availability in crops: A review. *Frontiers in Plant Science 11*, 590774. https://doi.org/10.3389/fpls.2020.590774

Sahnoun, M., Bejar, S., Sayari, A., Triki, M., Kriaa, M., & Kammoun, R. (2012). Production, purification, and characterization of two α-amylase isoforms from a newly isolated *Aspergillus oryzae* strain S2. *Process Biochemistry 47*, 18–25. https://doi.org/10.1016/j.procbio.2011.09.016

Steensels, J., Gallone, B., Voordeckers, K., & Verstrepen, K.J. (2019). Domestication of industrial microbes. *Current Biology 29*, R381–R393. https://doi.org/10.1016/j.cub.2019.04.025

Yang, D., Wei, H., Yang, X., Cheng, L.C., Zhang, Q., Li, P., & Mao, J. (2023). Efficient inhibition of *Aspergillus flavus* to reduce aflatoxin contamination on peanuts over Ag-loaded titanium dioxide. *Toxins 15*, 216. https://doi.org/ 10.3390/toxins 15030216

Yu, J.H. (2010). Regulation of development in *Aspergillus nidulans* and *Aspergillus fumigatus*. *Mycobiology 38*, 229–237. https://doi.org/10.4489/MYCO.2010.38.4.229

Wang, H., Chen, Q., Zhang, S., & Lu, L. (2021). A transient receptor potential-like calcium ion channel in the filamentous fungus *Aspergillus nidulans*. *Journal of Fungi 7*, 920. https://doi.org/10.3390/jof7110920

Watarai, N., Yamamoto, N., Sawada, K., & Yamada, T. (2019). Evolution of *Aspergillus oryzae* before and after domestication inferred by large-scale comparative genomic analysis. *DNA Research 26*, 465–472. https://doi.org/10.1093/dnares/dsz024

Wu, M.Y., Mead, M.E., Lee, M.K., Ostrem Loss, E.M., Kim, S.C., Rokas, A., & Yu, J.H. (2018). Systematic dissection of the evolutionarily conserved wetA developmental regulator across a genus of filamentous fungi. *mBio 9*, e01130–18. https://doi.org/10.1128/mBio.01130-18

Zhang, Y., He, J., Zheng, L., Jin, Z., Liu, H., Liu, L., Gao, Z., Meng, G., Liu, H., & Liu, H. (2022). Corrosion of aluminum alloy 7075 induced by marine *Aspergillus terreus* with continued organic carbon starvation. *NPJ Materials Degradation 6*, 27. https://doi.org/10.1038/s41529-022-00236-2